

Cycling Phosphorus on the Archean Earth: Part I. Continental weathering and riverine  
transport of phosphorus

Author: Jihua Hao<sup>1,2\*</sup>, Andrew H. Knoll<sup>3</sup>, Fang Huang<sup>4</sup>, Robert M. Hazen<sup>5</sup>, Isabelle Daniel<sup>1</sup>

\*Corresponding author: haojihua@gmail.com

<sup>1</sup>Univ Lyon, Université Lyon 1, Ens de Lyon, CNRS, UMR 5276 LGL-TPE, F-69622, Villeurbanne, France

<sup>2</sup>Present: Department of Marine and Coastal Sciences, Rutgers University, New Brunswick NJ 08901, USA.

<sup>3</sup>Department of Organismic and Evolutionary Biology, Harvard University, Cambridge MA 02138, USA

<sup>4</sup>Tetherless World Constellation, Rensselaer Polytechnic Institute, Troy NY, 12180, USA

<sup>5</sup>Geophysical Laboratory, Carnegie Institution for Science, Washington DC, 20015, USA

## **Abstract:**

Phosphorus (P) is the key nutrient thought to limit primary productivity on geological timescales. Phosphate levels in Archean marine sediments are low, but quantification of the P cycle and how it changed through a billion years of recorded Archean history remain a challenge, hindering our understanding of the role played by P in biosphere/geosphere co-evolution on the early Earth.

Here, we design kinetic and thermodynamic models to quantitatively assess one key component of the early P cycle – continental weathering – by considering the emergence and elevation of continents, as well as the evolution of climate, the atmosphere, and the absence of macroscopic vegetation during the Archean Eon. Our results suggest that the weathering rate of apatite, the major P-hosting mineral in the rocks, was at least five times higher in the Archean Eon than today, attributable to high levels of  $p\text{CO}_{2,g}$ . Despite this, the weathering flux of P to the oceans was negligible in the early Archean Eon, increasing to a level comparable to or greater than the modern by the end of eon, a consequence of accelerating continental emergence. Furthermore, our thermodynamic calculations indicate high solubilities of primary and secondary P-hosting minerals in the acidic weathering fluids on land, linking to high Archean  $p\text{CO}_{2,g}$ . Thus, weathering of P was both kinetically and thermodynamically favorable on the Archean Earth, and river water could transport high levels of dissolved P to the oceans, as also supported by the observed P-depletion in our new compilation of Archean paleosols. Lastly, we evaluated the relative rates of physical erosion and chemical weathering of silicates during the Archean Eon. The results suggest that continental weathering on the early and middle Archean Earth might have been transport-limited due to low erosion rates associated with limited subaerial emergence and low plateau elevations; by the late Archean, however, continental weathering would have transited to kinetically-limited state because of continental emergence, increased plateau elevation, and weakening weathering rates. Overall, our

weathering calculations together with paleosol evidence indicate an increasing flux of bioavailable P to the oceans through time, associated with late Archean continental emergence, reaching levels comparable to or higher than modern values by the end of the eon. Increased P fluxes could have fueled increasing rates of primary production, including oxygenic photosynthesis, through time, facilitating the irreversible oxidation of the Earth's atmosphere early in the Proterozoic Eon. (388 words)

**Keywords:** phosphorus; emergence of land; elevation of land; physical erosion; chemical weathering; paleosols (6/6)

## 1. Introduction

Phosphorus (P) is an essential bionutrient. Critical to the genetic material (nucleotides), membranes (phospholipids) and energy transfer (ATP) in cells, its availability is thought to limit primary productivity on geological timescales (Laakso and Schrag, 2018; Ruttenger, 2013; Tyrrell, 1999). Temporal variations in the P content of sedimentary rocks such as iron formation and carbonaceous shale suggest low levels of phosphate in Archean marine sediments (Bjerrum and Canfield, 2002; Planavsky et al., 2010; Reinhard et al., 2017), but quantification of the P cycle and how it changed through a billion years of recorded Archean history remain a challenge, hindering our understanding of the role played by P in biosphere/geosphere co-evolution on the early Earth.

The modern P cycle involves two dominant phosphate sources to the sunlit ocean: continental weathering and recycling in the oceans. Continental weathering provides the ultimate source of bio-available P to marine ecosystems, but due to the highly efficient recycling of organic matter in the modern oxidizing ocean, the flux of recycled P exceeds the continental input of P by two to three orders of magnitude (Schlesinger and Bernhardt, 2013). Thus, the high primary productivity of the modern ocean is sustained predominantly by recycled P. P burial on the other hand is determined by P input from continental weathering. On the early Earth, before the oxygenation of the atmosphere and ocean, recycling of organics in anoxic seawater might have been suppressed by a limited supply of oxidants (O<sub>2</sub>, sulfate, nitrate, and ferric iron) (Kipp and Stüeken, 2017; Laakso and Schrag, 2018), and P released to subsurface water masses might have been sequestered by reaction with ferrous iron to form vivianite (Derry, 2015). As a consequence, continental weathering might have accounted for a relatively larger proportion of total P supplied to primary producers in Archean oceans.

Continental input of P into early oceans, however, is poorly understood, for two major reasons. On the one hand, continental weathering of P might have been limited by less

extensive subaerial exposure of land and low elevations (Flament et al., 2013; Korenaga et al., 2017; Rey and Coltice, 2008), as well as a lower P content of early igneous rocks (Cox et al., 2018). On the other hand, high levels of atmospheric CO<sub>2,g</sub> thought to characterize the early Earth favor weathering and riverine transport of phosphorus (Hao et al., 2017a). In addition, the absence of macroscopic vegetation on Archean continents should also have affected both chemical and physical weathering relative to the modern Earth.

Despite these challenges, there have been a few attempts to estimate the continental flux of P into Archean oceans. Hao et al. (2017a) used a thermodynamic model to simulate the maximum solubilities of apatite (Ca<sub>5</sub>(PO<sub>4</sub>)<sub>3</sub>(OH,F,Cl)), the major P-hosted mineral in the crust, in proposed Archean weathering fluids; however, they could not quantify continental fluxes because they lacked terms for weathering kinetics, the growth and elevation of continental land, and the evolution of climate and atmosphere. Recent studies have placed constraints on the parameters that collectively govern these fluxes, including continental emergence *per se* (Flament et al., 2013; Korenaga et al., 2017), atmospheric composition (Krissansen-Totton et al., 2018), and temperature (Krissansen-Totton et al., 2018). Despite uncertainties, these estimates enable us, for the first time, to quantify continental input of bioavailable P to Archean oceans. Here we design kinetic and thermodynamic models to estimate the continental weathering of apatite and riverine transport of P, incorporating the emergence and elevation of continental land, atmospheric composition, climate, and the absence of vegetation.

## **2. Important environmental parameters controlling phosphorus weathering**

Continental weathering of phosphorus depends on a number of environmental factors, all of which have evolved through the Earth history.

### ***2.1 Emergence of land***

Although the volume of continental crust might have increased more or less continually early in Earth history (Hawkesworth and Kemp, 2006; Roberts and Spencer, 2015), only limited evidence exists for emergent land before the middle Archean Eon. Various lines of evidence, including stratigraphic observations, geophysical simulations, and geochemical data agree that the early and middle Archean continents had only limited subaerial exposure (Arndt, 1999; Campbell and Davies, 2017; Ernst et al., 2016; Flament et al., 2013, 2008; Korenaga et al., 2017; Kump and Barley, 2007; Molnar, 2018; Trower and Lowe, 2016).

For example, the 3.5-3.26 Ga Onverwacht Group, South Africa, contains some ten kilometers of stratigraphy, but nearly all of it is volcanic, and much consists of pillow basalts extruded below sea level (Lowe and Byerly, 1999). With one exception, detrital zircons suggest that such clastic sedimentary rocks as are preserved derive largely from regional volcanics (Drabon et al., 2017). The exception is a three meter sandstone bed near the top of the Onverwacht succession that contains zircons older than 3.8 Ga. These suggest that older differentiated crust existed but was rarely eroded (Byerly et al., 2018). Clastic sedimentary rocks are more abundant in the 3.26-3.22 Ga Fig Tree Group, but the lithic grains that dominate these lithologies again speak to reworking of regional volcanics (Nocita, 1989). Only with deposition of the immediately overlying Moodies Group do we see accumulations of quartz-rich sandstones derived from exposed continental crust. Later Archean basins increase in lateral dimensions, culminating in the latest Archean Transvaal basin, whose spatial scale suggests accumulation along the margin of a large, stable craton (Knoll and Beukes, 2009). Similar features characterize Archean stratigraphy in Western Australia (e.g., van Kranendonk, 2006).

Geochemical data also support late emergence models. End-Archean increase in the  $^{87}\text{Sr}/^{86}\text{Sr}$  of carbonate rocks was originally thought to reflect continental growth (Taylor and McLennan, 1985) or continental igneous rock composition (Bataille et al., 2017), but is equally well explained in terms of late continental emergence (Flament et al., 2013; see also Pons et

al., 2013, for a comparable perspective based on Zn isotopes). Indeed, interpretation in terms of emergence helps greatly to reconcile otherwise conflicting stratigraphic and geochemical inferences about continental growth on the Archean Earth. Consistent with this view, Bindeman et al. (2018) and Spencer et al. (2019) have both interpreted the oxygen isotope record in terms of late Archean continental emergence, while Kump and Barley (2007) have argued for an increase in subaerial volcanism near the Archean-Proterozoic boundary. We know of no comparable suite of evidence favoring much earlier emergence of stable continents.

Lee et al. (2018) recently proposed a scenario in which pronounced continental emergence developed only near the end of the Proterozoic Eon, catalyzing late Neoproterozoic climatic and redox transformations. This proposal is at odds with several lines of geochemical evidence documenting large continental weathering and erosional fluxes by late Archean times (Bindeman et al., 2018; Satkoski et al., 2016; Viehmann et al., 2018), not to mention thousands of meters of quartzose sandstones in earlier Proterozoic basins around the world. If all land were submerged, there would be no depletion of P during seafloor weathering, which is inconsistent with Archean paleosol records (**Fig. 6**). Moreover, in the warm climate suggested by biogeochemical models for a land-free Archean (Krissansen-Totton et al., 2018), rapid precipitation of vivianite would remove essentially all available P from seawater. Thus, any scenario with essentially no exposed land mass implies minimal global primary production sustained by limited fluxes of P from extraterrestrial sources (Pasek and Lauretta, 2008; Tsukamoto et al., 2018), inconsistent with evidence for substantial biological activity in the Archean ocean. Taken together, sedimentary and geochemical evidence make protracted late Archean continental emergence a more plausible scenario.

Quantification of continental emergence depends on a number of parameters, none of them well constrained. These include mantle temperature, crustal composition – and hence buoyancy, seawater volume, modes and rates of tectonic activity, and continental hypsometry

(Korenaga et al., 2017). Previous studies of the Archean Earth have rarely incorporated all of these parameters; indeed, parameter selection has commonly seemed arbitrary. For this paper, we chose three models for secular change in continental emergence from two recent studies (**Fig. 1a**) (Flament et al., 2013; Korenaga et al., 2017). Among the available estimates, we suggest that these provide the best understanding of continental emergence available at present. Moreover, because they incorporate multiple models of continental growth and mantle devolatilization/revolatilization, these papers provide a broad range of possible histories.

Apart from more limited emergence of the Archean continents, a hotter and more buoyant Archean mantle could not support high plateau elevations (Fig. 1b; Flament et al., 2013; Rey and Coltice, 2008), although the actual elevation should depend on a balance between tectonic uplifting and exhumation/erosion. Based on the classic Culling's model (Culling 1960, 1963), the erosion rates is linearly proportional to topographic slope, which depends on relative elevation. Physical erosion is responsible for the removal of sediment and exposure of fresh rock surface for chemical weathering. We further simplify Culling's model by assuming that physical erosion is proportional to the elevation of land, i.e.,  $E_r \propto H$ , an approach that has previously been applied to macroscale erosion processes (Lee et al., 2015; Jadamec et al., 2007). Thus, physical erosion on the Archean Earth was probably limited by the low elevation of continental land, as well as its limited aerial extent, as investigated below.

## 2.2 *P content of rocks*

The P content of erodible rocks is another important factor in estimating the weathering flux of P. P content depends on rock composition (Porder and Ramachandran, 2013; Ronov, 1982) and exposure through geological time (Cox et al., 2018). On the modern Earth, the exposure area of sedimentary rocks exceeds that of volcanics (Bluth & Kump, 1991). Thus, on the modern Earth, the contribution of sedimentary rock weathering to continental P flux can



potentially be substantial (Hartmann et al., 2014). On the early Archean, however, this sedimentary reservoir might have been less important. The P content of sedimentary rocks varies widely and can be either higher or lower than that of ultramafic-mafic volcanic rocks (Porder & Ramachandran, 2013; Ronov, 1982), which were the major crustal lithologies in the Archean Eon. Quantification of the contribution of sedimentary rock weathering to P flux needs to consider relative P content, surface exposure, and weathering kinetics of sedimentary vs. volcanic rocks. Collectively, the resultant uncertainty may become too large to yield any useful implications. It is also possible that agpaitic rocks, which are unusually rich in phosphorus, could add complexity to weathering and erosional P fluxes; however, all known examples of agpaitic rocks postdate the Archean (Marks and Markl, 2017). With these unknowns and uncertainties in mind, we instead chose to use relative P content of crust in the Archean and modern Earth. A compilation of more than 176,000 igneous rock samples indicates that the P content of the Archean crust was perhaps half that estimated for today, although felsic rocks show no pronounced secular trend (Cox et al., 2018).

### *2.3 Archean atmospheric composition*

Acidity and redox state are two more important controls on the chemical dissolution of phosphorus. Rainwater acidity is controlled by the dissolution of atmospheric CO<sub>2</sub> and deprotonation of H<sub>2</sub>CO<sub>3</sub>. It has been generally proposed that high levels of CO<sub>2</sub> are required to compensate the weaker young sun (20 to 30 % lower luminosity) (Gough, 1981) and sustain a temperate climate in the Archean. As a result, Archean rainwater is estimated to have been more acidic than modern (Hao et al., 2017a). Log dissolution rate of the major P-hosted minerals, i.e. apatite, has been experimentally shown to increase linearly with decreasing pH (Guidry and Mackenzie, 2003). The solubility limits of P-minerals also depend significantly on pH, as investigated below.

The redox state of the Archean atmosphere and surface waters is thought to have been weakly reducing (Hao et al., 2019). Under these conditions, ferrous iron is stable rather than the ferric iron that generally forms in modern oxidizing weathering reactions. Given the much greater solubility of ferrous iron relative to ferric iron, Archean weathering should result in Fe-depletion, as evidenced by the paleosol record (Rye and Holland, 1998) and thermodynamic simulation (Hao et al., 2017b). Today, the largest proportion of the reactive phosphorus pool in riverine transport is Fe-bound phosphorus, because during oxidative weathering Fe(II) is oxidized to Fe(III), leading to the formation of Fe(III)-(hydr)oxide or Fe(III)-coated clay minerals that have a high surface adsorption affinity for phosphate (House, 2003; Withers and Jarvie, 2008). This surface retention of P is thought to be a key process limiting dissolved P levels in modern river water. However, we expect there would have been little Fe-bound inorganic phosphate in anoxic Archean river water and, correspondingly, high concentrations of dissolved inorganic phosphate. Below we examine whether or not the acidic and anoxic weathering fluids could transport high concentrations of dissolved phosphate on the Archean Earth.

#### *2.4 Absence of vegetation*

The presence of land plants affects both chemical weathering and physical erosion. On the one hand, vegetation is thought to facilitate chemical weathering through the secretion of organic ligands that attack primary minerals (Neaman et al., 2005) and/or elevation of soil  $p\text{CO}_{2,g}$  by means of microbial decomposition of organic debris in the soil (Berner, 2004). Overall, the presence of non-microbial vegetation is proposed to accelerate the chemical dissolution of primary minerals by a factor of 3 to 4, as calculated by cation release from vegetated vs. barren areas (Berner et al., 2004). The enhancing factor of 4 is further supported by attempts to match the COPSE model to multiple Phanerozoic paleo-weathering proxies

(Lenton et al., 2018). On the other hand, vegetation can protect substrates from physical erosion and thus hinder the exposure of fresh rock for further weathering, particularly where removal of the soil cover is not efficient (Berner, 2004). It has been shown that vegetation cover ( $VC\%$ ) has a negative exponential correlation with soil erosion rate (Gyssels et al., 2005); i.e.,  $E_r \propto \exp(-b*VC)$ , where  $b$  is an exponential constant. Modern Earth has approximately 60% vegetation cover; whereas, none was present on the Archean Earth. Absence of vegetation on the Archean Earth might compensate partially for the effect of low plateau elevation.

### 3. Methods and Materials

#### 3.1 Chemical weathering model

We modeled the chemical weathering of silicates using the geological carbon cycle model of Krissansen-Totton et al. (2018), with two modifications. First, we used three models for the emergence of land above sea level as introduced above rather than the estimates of continental growth used in Krissansen-Totton et al. (2018). Second, because there was no macroscopic vegetation on the Archean Earth, we set the vegetation compensating factor as 0.25 rather than 0.1 to 1, randomly sampled over the Precambrian in the original model. We kept all other parameters as in the original code.

The dissolution rate of apatite ( $R$ ) has been proposed (Guidry and Mackenzie, 2000) to be:

$$R = A * \exp\left(-\frac{E_a}{R_g T}\right) * [H^+]^{n_H} \quad (1)$$

$R$ : mole/(cm<sup>2</sup>\*s);  $A$ : reaction constant, mole/(cm<sup>2</sup>\*s);  $E_a$ : activation energy of dissolution (34.7 kJ/mole) (Guidry and Mackenzie, 2003);  $R_g$ : universal gas constant, 0.008 kJ/(mole\*K);  $T$ : temperature, K;  $[H^+]$ : activity of hydrogen ion in the weathering fluid;  $n_H$ : reaction order (0.81 at  $2 < \text{pH} < 5.5$ ) (Guidry and Mackenzie, 2003).

Eqn. 1 has been used to estimate continental inputs of P during the past 600 Ma (Guidry and Mackenzie, 2000). Guidry and Mackenzie (2000) assumed a constant  $[H^+]$  of  $10^{-5}$  for soil waters throughout this interval; however, the log dissolution rate of apatite can decrease linearly with pH at  $pH < 6$  (Guidry and Mackenzie, 2003). Due to high levels of  $CO_{2,g}$  in the Archean atmosphere, weathering fluids would have been generally acidic (Hao et al., 2017a). Thus,

$$\frac{R_{Archean}}{R_{Modern}} = \exp \left[ -\frac{E_A}{R_g} \left( \frac{1}{T_{Archean}} - \frac{1}{T_{Modern}} \right) \right] * \left( \frac{H_{Archean}^+}{H_{Modern}^+} \right)^{n_H} \quad (2)$$

At acidic pH,  $[H^+]$  of rainwater varies approximately with the partial pressure of  $CO_{2,g}$  ( $P_{CO_{2,g}}$ ):

$$[H^+]^2 = K_1 * K_{CO_2} * P_{CO_{2,g}}$$

$$[H^+] = K * \sqrt{P_{CO_2}} \quad (3)$$

where  $K = \sqrt{K_1 * K_{CO_2}}$ ;  $K_1$  represents the first deprotonation constant of carbonic acid;  $K_{CO_2}$  represents the solubility constant of  $CO_{2,g}$  in water under ambient conditions.

It is notable that the pH of weathering fluids would have increased as weathering progressed due to release of alkalinity from the alteration of silicate and carbonate minerals. However, as shown in Hao et al. (2017a), the pH increment from rainwater (starting weathering fluid) to river water (ending weathering fluid) is similar at different levels of  $pCO_{2,g}$ ; i.e.

$\frac{H_{Archean}^+}{H_{Modern}^+}$  of weathering fluids should depend primarily on  $\frac{pCO_{2,g,Archean}}{pCO_{2,g,Modern}}$ . Apart from the

dissolution of  $CO_{2,g}$ , introduction of organic acids as well as  $SO_x$  and  $NO_x$  gases may affect the acidity of rainwater, particularly in some local environments or during particular geologic periods. However, deposition of  $SO_x$  and  $NO_x$ , which are mostly anthropogenic today, might have been insignificant for the preindustrial times, let alone for the Archean Eon. The overall effects of organic acids, which mainly come from macroscopic vegetation today, were considered in our model as discussed below.

Consequently, the relative chemical weathering rate of apatite is

$$\frac{R_{Archean}}{R_{Modern}} = \exp \left[ -\frac{E_A}{R_g} \left( \frac{1}{T_{Archean}} - \frac{1}{T_{Modern}} \right) \right] * \left( \frac{P_{CO_2,Archean}}{P_{CO_2,Modern}} \right)^{\frac{n_H}{2}} \quad (4)$$

Recently, Krissansen-Totton et al. (2018) reconstructed the evolution of Archean surface environments, including  $pCO_{2,g}$  and temperature, based on a model for the geological carbon cycle. Here, we incorporate the weathering kinetics of apatite (eqn. 4) into Krissansen-Totton et al.'s model and use their output of  $pCO_{2,g}$  and temperature of each run to calculate the weathering kinetics of phosphorus as it changed through the Archean Eon.

We developed three versions of our model, reflecting hypotheses for early, intermediate and late continental emergence (Fig. 1a). All generate results that are similar in trajectory, albeit different in timing. While the question of when and to what extent continents emerged above sea level remains a topic for debate, we believe there are compelling reasons to favor late emergence hypotheses, as proposed in models that relate the water cycle (Korenaga et al., 2017) and continental hypsometry (Rey and Colitce, 2008) to a secular decline in mantle temperature through the Archean Eon. Based on sedimentary and geochemical evidence (Sec. 2.1), we favor large-scale subaerial emergence of continents in the late Archean Eon as the most likely scenario. As we discuss below (**Discussion**), weathering of P on early and middle Archean continents might have also been suppressed by slow physical erosion due to the low elevation of emergent land masses.

Lastly, vegetation has been shown to accelerate chemical weathering by a factor of about 4 (Berner, 2004; Lenton et al., 2018); thus, the weathering kinetics of apatite are divided by 4 to compensate for the effect of no vegetation in the Archean.

The total flux ( $p$ ) of P by continental weathering is

$$p(t) = SA * R \quad (5)$$

SA: global surface area of apatite available for weathering.

Therefore,

$$\frac{p(Archean)}{p(Modern)} = \frac{SA_{Archean} * R_{Archean} * C(P)_{Archean}}{SA_{Modern} * R_{Modern} * C(P)_{Modern}} \quad (6)$$

$C(P)$ : content of P in the rock. Here, the ratio of  $SA * C(P)$  was used to approximate the relative exposure of apatite minerals for chemical weathering on exposed Archean and modern continents.

For simplicity, we assumed an average P content for Archean land equal to half the modern value, i.e.  $C(P)_{Archean}/C(P)_{Modern} = 1/2$ . This assumption is within the range of values reported in Cox et al.'s compilation (Cox et al., 2018). Regardless of the uncertainties in this estimate, we consider the evolution of crustal P content to be less important for the continental transport of reactive P than weathering rate and continental growth and emergence (Flament et al., 2013; Korenaga et al., 2017). As in Krissansen-Totton et al. (2018), the weathering model was run 10,000 times to build distributions for model outputs.

Due to lack of a universal value for the weathering rate of apatite on the modern Earth, we calculated only the relative weathering rate of apatite on the Archean Earth compared to preindustrial time using Eqn. (4) (**Figs. 2-4**). Similarly, we calculated only the relative chemical dissolution flux of P using Eqn. (6), due to the fact that the speciation of P in reducing and acidic Archean river water might have differed substantially from that of preindustrial rivers (*Sec. 4.2* and **Table 2**).

### 3.2 Physical erosion

As mentioned above, elevation and vegetation are two major factors controlling rates of physical erosion:

$$\frac{E_{r,Archean}}{E_{r,Modern}} = \frac{H_{Archean}}{H_{Modern}} \times e^{-b(VC_{Archean} - VC_{Modern})} \quad (7)$$

Reported  $b$  values vary significantly and this variation strongly affects the calculated effectiveness of vegetation on the protection of soil from erosion (Gyssels et al., 2005). Here,

we adopt a range of  $b$  values from 0.02 to 0.04, representing the range of literature values (Gyssels et al., 2005). With no information of actual Archean plateau elevations, we chose to apply Flament et al.'s (2013) reconstructed maximum plateau, which should approximate an upper limit on actual elevations. The vegetation coverage in the Archean ( $VC_{\text{Archean}}$ ) is set to be 0 and modern ( $VC_{\text{Modern}}$ ) to be 60%.

### *3.3 Thermodynamic calculations of P-minerals' solubilities*

Solubility limits for primary and secondary phosphate minerals in Archean river water and seawater were calculated using the equilibrium constants of their dissolution reactions under ambient conditions (25 °C and 1 atm) (**Table 1**). Based on previous studies, we made various assumptions about concentrations for ions other than phosphate.

For our reconstruction of Archean river water, F- concentration was assumed to be equal to that of modern river water; i.e.,  $1.3 \times 10^{-8}$  mole/L (Deshmukh et al., 1995) although the actual level is unknown. This simple consideration might over- or under-estimate the solubility limits of F-bearing phosphates. However, our calculations suggest that the F-bearing phosphates are highly soluble in the Archean weathering fluids (**Fig. 5a and b**) and the results are still valid even with orders of magnitude higher or lower levels of fluorine. Due to high levels of  $CO_{2,g}$ , Archean river water is expected to have been more acidic than at present (Hao et al., 2017b). Acidity of the weathering fluid also depends on the extent of reactions with silicate and carbonate minerals, increasing at high reaction extent due to the release of alkalinity by rock alteration. Here, we investigated a wide range of Archean  $pCO_{2,g}$  values (1 to  $10^{-2.5}$  bar) from Krissansen-Totton et al. (2018) and modeled the corresponding chemistry of Archean river water using a previously reported late Archean weathering model (Hao et al., 2017b). The outputs, particularly pH and aqueous activity of  $Ca^{2+}$ ,  $Fe^{2+}$ ,  $Cl^-$ , and  $SiO_{2,aq}$  (**Table S1**), were used to calculate the solubilities of primary and secondary P-minerals, based on the reported

thermodynamics of these minerals (**Table 1**). As for the solubilities of variscite ( $\text{AlPO}_4 \cdot 2\text{H}_2\text{O}$ ) and strengite ( $\text{FePO}_4 \cdot 2\text{H}_2\text{O}$ ), Al(III) and Fe(III) levels were assumed to be limited by the solubility of their corresponding amorphous hydroxides. However,  $\text{Fe}(\text{OH})_3$  is not believed to have precipitated widely during Archean weathering, as supported by observations of Fe-depletion in Archean paleosols (Rye and Holland, 1998). Therefore, the solubility of strengite, although calculated in this study, should serve only as a lower limit on Archean river water.

### 3.4 P-weathering in paleosol record

Paleosol selection for our analysis is based mainly on standards proposed by Rye and Holland (1998), augmented by more recent additions. **Table S2** lists all data sources.

The enrichment index of P is defined as:

$$\Delta\left(\frac{P}{Ti}\right) = \frac{\left(\frac{P}{Ti}\right)_{\text{Paleosol}} - \left(\frac{P}{Ti}\right)_{\text{Bedrock}}}{\left(\frac{P}{Ti}\right)_{\text{Bedrock}}} \quad (8)$$

$\Delta(\text{P/Ti}) > 0$  indicates enrichment of P during weathering whereas  $\Delta(\text{P/Ti}) < 0$  indicates depletion of P. Since positive values of  $\Delta(\text{P/Ti})$  reflect the addition of P to the paleosols, most likely by mineral aerosols, we decided to use only negative  $\Delta(\text{P/Ti})$  values for Student's t-test (**Fig. 6**). **Fig. S4** presents all  $\Delta(\text{P/Ti})$  values and the corresponding statistical results.

## 4. Results

### 4.1 Continental weathering of phosphorus

As noted above, we have applied three cases of land emergence to simulate ratios of apatite dissolution rate (rate per unit area, e.g. mole/cm<sup>2</sup>\*s in this study; Figs. 2a-4a) and P weathering flux (Figs. 2b-4b) through the Archean Eon relative to modern.

In the case of slow late Archean emergence of land (Flament et al., 2013), the relative weathering rate of apatite decreases slowly but monotonically through the Archean Eon (**Fig. 2a**), largely due to the secular decline of  $\text{pCO}_{2,\text{g}}$  (**Fig. S1**). When we compensate for a lack of



vegetation, the apatite dissolution rate is always greater than five times the modern, indicating that dissolution of apatite was kinetically favorable under the acidic conditions of the Archean land surface. However, the relative weathering flux of P remains negligible until 3.5 Ga, when land starts to emerge and then increases rapidly (**Fig. 2b**), reaching a value ranging from 0.25 to 1 by the end of the Eon. The increase in weathering flux is largely ascribed to the late Archean emergence of land, which more than compensates for the declining weathering rate of apatite. However, continental weathering flux of silicates simulated by Krissansen-Totton et al. (2018) decreased slightly through the Archean Eon (Fig. 3E in Krissansen-Totton et al., 2018). This lack of synchronization is due to the different settings of land fraction (relative to the modern land area). In their simulations, Krissansen-Totton et al. (2018) assumed 0-75% land fraction emergence above sealevel and no change with time during the Archean Eon. Under these circumstances, decreasing  $p\text{CO}_{2,g}$  and temperature (Fig. 3B & D in Krissansen-Totton et al., 2018) would inevitably result in a decreasing continental flux of silicate weathering. As argued by Krissansen-Totton et al. (2018), the degree of land emergence has only a minor influence on the evolutionary history of seawater pH and climate, the foci of their study. However, the geologic history of land emergence as discussed in Sec. 2.1 is highly relevant to the estimation of continental weathering flux. For this reason, we used reconstructed histories of Archean land emergence (Fig. 1a) as inputs into our weathering model, which shows an increasing continental flux of P through time. In **Fig. S1-3**, we also displayed our reconstructed evolution of continental silicate weathering, which shows increasing flux as well, consistent with other geochemical studies. These increasing fluxes of continental weathering are mainly driven by the land emergence.

In the second case, where land emerged rapidly from the middle Archean (Korenaga et al., 2017), the trends of relative weathering rate and flux are similar to the case described above (**Fig. 3**). That said, the relative weathering rate of apatite decreases to even lower levels toward

the end of the Archean (**Fig. 3a**) compared with the slow emergence case. This difference lies in the lower levels of  $p\text{CO}_{2,g}$  and temperature, a consequence of stronger continental weathering on a larger land surface in the late Archean Eon (**Fig. S2**). Similar to the first case, the relative chemical weathering flux of P increases from the middle Archean and reaches a value close to or higher than 1 by the end of the Archean, representing a flux comparable to or higher than the modern value (**Fig. 3b**), again because of continental emergence.

In the last case, where land started emerging early in the Archean Eon (Korenaga et al., 2017), the relative weathering rate of apatite once again declines monotonically with time (**Fig. 4a**). The relative weathering flux of P, however, increases rapidly from the early Archean, reaching a plateau value of 0.5 to 4 in the middle Archean (3.5 Ga) before decreasing slightly into the late Archean (**Fig. 4b**). This trend differs from two cases discussed above, mainly due to the rapid emergence of land in the early Archean. The declining weathering flux is largely ascribed to the declining weathering rate of apatite. In this case, the weathering flux of P is comparable to or higher than the modern level since the middle Archean. However, as mentioned earlier, we believe this case of early land emergence is not well supported by sedimentary and geochemical evidence. Additionally, on the early-middle Archean Earth, continental weathering, although chemically favorable, might have been severely limited by low rates of physical erosion, reflecting the low mean elevation of continental land (**Fig. 1b**), as elaborated in **Discussion**.

In summary, given three different cases of land emergence, Archean chemical weathering of apatite is always kinetically more favorable than today, and the weathering flux of P is predicted to have reached levels comparable to today at least by the end of the Archean Eon.

#### *4.2 Riverine transport of phosphorus*

Today, continental weathering of P-hosting minerals generates various forms of phosphorus. Among these, detrital particulate phosphorus is the largest component but is not biologically available to the marine ecosystem. Bioavailable phosphorus, also known as ‘reactive’ phosphorus, is composed of dissolved inorganic phosphorus (DIP), dissolved organic phosphorus (DOP), particulate organic phosphorus (POP), Fe-bound inorganic phosphorus (PIP, Fe-bound), and about 20% aeolian phosphorus (desorption from aeolian dusts) (Compton et al., 2000). The largest proportion of the reactive phosphorus pool is Fe-bound phosphorus, because during oxidative weathering Fe(II) is oxidized to Fe(III), leading to the formation of Fe(III)-(hydr)oxide or Fe(III)-coated clay minerals that have a high surface adsorption affinity for phosphate (House, 2003; Withers and Jarvie, 2008). This surface retention of P is thought to be a key process limiting dissolved P levels in modern river water. However, in the Archean, when the atmosphere was anoxic and weakly reducing, weathering is thought to have leached Fe(II) without oxidation, as supported by the previously noted Fe-depletion in Archean paleosols (Rye and Holland, 1998). Therefore, we expect that there would have been little Fe-bound inorganic phosphate in Archean river water and, correspondingly, a higher concentration of dissolved inorganic phosphate (**Table 2**). Moreover, due to higher levels of atmospheric CO<sub>2</sub>, Archean weathering fluids, including rainwater and river water, are thought to have been more acidic than today (Hao et al., 2017a). As presented in **Fig. 5a and b**, acidic and reducing Archean weathering fluids allow much higher solubilities of primary and secondary P-bearing minerals than dissolved P levels in modern river water at a wide range of pH values (4.5 – 7.5) (Gaillardet et al., 2014). Indeed, the dissolution of P-minerals in Archean acidic waters is both kinetically and thermodynamically more favorable than today. High solubility of phosphate in Archean river water would enable riverine transport of rapidly weathered phosphate to the sea(s).

Based on **Fig. 2b-4b**, the continental weathering flux of phosphorus in the late Archean was 0.3 to 3.5 times the modern value. In this study, we assumed that the total dissolved inorganic phosphate in Archean river water was the sum of modern DIP and Fe-bound PIP multiplied by the ratio of chemical weathering flux ( $p$ ) between the Archean and modern (**Table 2**). Similarly, we assumed that chemical weathering of organic P from sedimentary rock (DOP and POP) and the physical weathering of phosphate (detrital and aeolian P) are influenced primarily by the relative weathering area (**Table 2**). However, this simple consideration might over- or under-estimate the contribution of these components. For example, physical weathering is dependent on many environmental factors, including elevation, climate, and vegetation (Drever, 1994; Edmond et al., 1995; Zhou et al., 2008). In the Archean, these all differed from today (see **Discussion**), complicating estimates of detrital and aeolian P fluxes on the early Earth. Similarly, the weathering of organic P depends on a number of environmental factors, including the redox state of weathering fluids, the content of organic-P in sedimentary rock, and the presence of life. For example, organic matter should have had a longer retention time in anoxic Archean environments compared to today. Thus, organic P, once weathered, might have been stably transported in reducing Archean waters. Empirical analyses, however, show that the P content of Archean shales is lower than that of their modern counterparts (Reinhard et al., 2017). Regardless of these uncertainties, the contributions of organic and aeolian components to overall riverine fluxes would have been relatively small compared with the combined fluxes of dissolved inorganic and Fe-bound P. We note again that detrital P, although representing the largest proportion of continental P, is not biologically available. Therefore, we believe that our calculations provide a reasonable estimate of the continental input of bioavailable P to the Archean ocean.

Direct evidence of P-behaviors during Archean weathering comes from the paleosol record. The mobility of P in paleosols was assessed as the ratio of P to the immobile element

Ti (relative to underlying bedrock) (**Methods and Materials**). To minimize the effect of post-depositional processes, we focused on long term trends in the mean level of P/Ti, a method applied widely in interpretations of ancient sediments (Cox et al., 2018; Planavsky et al., 2010; Stüeken et al., 2012). The result (**Fig. 6 & S4**) shows stronger depletion of P in Archean paleosols compared with younger examples. In addition, a Student's t-test of P/Ti in Archean and post-Archean paleosols confirms that Archean paleosols are significantly more depleted in P than their post-Archean counterparts ( $p < 10^{-4}$ ) (**Fig. 6b & S4b**). These results are qualitatively coherent with the outputs of our weathering models, which indicate more pronounced weathering of P in the Archean relative to the modern Earth.

## 5. Discussion

Continental weathering is generally classified as either kinetically- or transport-limited, depending on relative rates of chemical weathering and physical erosion (West et al., 2005). For kinetically-limited weathering, the rate of physical erosion exceeds the rate of chemical weathering; total weathering flux is then limited by the chemical weathering supply. In the case of transport-limited weathering, the rate of chemical weathering depends on exposure of fresh rock by physical erosion; total weathering flux is limited by the removal of regolith by physical erosion. Climate and tectonics are two major factors controlling these weathering scenarios.

Considering the high atmospheric  $p\text{CO}_{2,g}$  of Archean Earth (Hart, 1978; Kasting et al., 1989; Krissansen-Totton et al., 2018; Owen et al., 1979), chemical weathering of silicates should have been more rapid than in the modern environment (Berner, 2004). In contrast, physical erosion of Archean continents might have been limited by the restricted area and low elevation of mountainous areas. Geophysical models indicate that hot Archean continental lithosphere could not support mountains with high elevations (Flament et al., 2013; Rey and Coltice, 2008). Specifically, the maximum elevation of continental plateaus might have

increased from around 1000 to 3900 m (**Fig. 1b**) as the mantle cooled through Archean time, in contrast to 5500 m for present-day Tibet (Flament et al., 2013). The elevation of mountainous areas has long been proposed to control maximum erosion fluxes (Edmond et al., 1995). Vegetation cover is another important factor that strongly affects erosion (Gyssels et al., 2005). In order to decipher whether Archean weathering was kinetically or transport limited, we adopted models from the literature to quantify the relative rates of silicate weathering and physical erosion (**Methods and Materials**).

The result (**Fig. 7**) shows an increasing rate of physical erosion but decreasing rate of chemical weathering from the early to late Archean Eon. During the Archean, the maximum elevation of mountainous areas increased through time, as did the total area of emergent crust (Flament et al., 2013; Korenaga et al., 2017), resulting in enhanced physical erosion. At the same time, declining  $p\text{CO}_{2,g}$  and temperature would have led to decreasing rate of chemical weathering. The absence of vegetation in the Archean could have strengthened physical erosion because of the lack of sediment protection (Drever, 1994); on the other hand, weakened chemical weathering (Berner, 2004) would have had the opposite effect. The no-vegetation effect, however, remained constant throughout the Archean and, hence, makes no contribution to rate changes within the Eon.

In all three scenarios, the system begins in a predominantly transport-limited regime and transitions to one of largely kinetic limitation, with the time of cross-over depending on the model for continental emergence. Thus, in our preferred scenario, high rates of chemical weathering were favored by early and middle Archean conditions (**Fig. 2-4**), but continental flux of P to the oceans would have been limited by slow physical erosion and the limited exposure of fresh rock. It is notable that our model input of elevation represents the maximum elevation of Archean plateaus reconstructed by Flament et al. (2013). The actual elevation might have been much lower, indicating even slower erosion rates. As relative rates of physical

erosion increased, they came to exceed the relative rate of chemical weathering in the late Archean (3.0 to 2.5 Ga) (**Fig. 7**). From then on, continental flux of P was dominated by the flux of chemical weathering (**Fig. 2b-4b**). On the modern Earth silicate weathering is transport-limited in catchments such as continental cratons while kinetically limited in alpine and submontane catchments (West et al., 2005). On the global scale, Hartmann et al. (2014) estimated the effect of soil on chemical weathering flux and suggested a 40 % reduction by soil shielding compared to an Earth surface covered by young rocks. Nevertheless, our calculated relative rate of physical erosion could exceed that of chemical weathering by several-fold on the late Archean Earth (**Fig. 7**), marking a notable transition from large-scale transport-limited weathering in the early and middle Archean to kinetically-limited weathering in the late Archean Eon. This result confirms our flux calculations, which indicate that continental weathering could have contributed comparable or higher amounts of bioavailable phosphorus to the late Archean ocean ecosystem than occurs today.

## **6. Conclusions**

Chemical weathering depends on several factors that have changed through time, including temperature, pH, vegetation cover, and the chemical composition, exposed area, and elevation of land masses. Given high but decreasing  $p\text{CO}_2$  in the Archean atmosphere, rates of apatite weathering should have been high early in the Archean and then decreasing through the duration of the eon. Despite the high apatite weathering rates dictated by relatively acidic rainwater, P fluxes from the continents to the oceans were probably very low in the early Archean because of limitations in the exposed surface area and elevation of continents. As continents emerged through time, P fluxes to the oceans would have increased, reaching values comparable to the modern by the end of the eon.

We have modeled secular changes in P fluxes in relation to three distinct models for continental emergence. Not surprisingly, they give results that differ in timing but agree in overall trend. Increasingly, stratigraphic, geophysical, and geochemical data support strong continental emergence in the late Archean Eon (Bindeman et al., 2018; Flament et al., 2013, 2008; Spencer et al., 2019), favoring a variant on the model results shown in **Figure 1**. Depending on the exact time scale of continental emergence, the major increase in P flux to the ocean could have occurred close to the Archean-Proterozoic boundary.

Such a history has a number of implications for primary production early in Earth history. Among other things, the inferred time trajectory of P flux to the oceans lessens the need for models that posit the evolution of oxygenic photosynthesis just before the Great Oxidation Event at ca. 2.4 Ga. Even if oxygenic phototrophs (cyanobacteria) existed in early Archean oceans, rates of primary production might have been too low to affect atmospheric oxygenation. Also, above a critical level of Fe/P in the oceans, anoxygenic photoautotrophs would have been favored ecologically over oxygenic photoautotrophs in most parts of the Archean biosphere (Jones et al., 2015), which could account for the carbon mass balance inferred from carbon isotopes (Krissansen-Totton et al., 2015) without producing O<sub>2</sub>. Transiently high oxygen production – and consequently, “oxygen oases” – would have been possible locally where P availability was high and/or the availability of alternate electron acceptors for photosynthesis was low. Molecular phylogenies that place the origin of oxygenic photosynthesis in freshwater (Blank and Sanchez-Baracaldo, 2010) are consistent with this reasoning and our model results. And, as others have argued (e.g., Flament et al., 2008; Campbell and Davies, 2017), increased P fluxes associated with late Archean continental emergence could have fueled the relatively high rates of oxygenic photosynthesis needed to nudge Earth’s surface into a permanently oxic state.



578 **Acknowledgements** We thank Dimitri A. Sverjensky, David Catling, Cin-Ty Lee, Nicolas  
579 Coltice, Ciaran Harman, Mathew Pasek, Michael Kipp, Lu Pan, and Chao Liu for helpful  
580 discussions, and two anonymous reviewers and Tim Lenton for constructive comments. JHH  
581 and ID thank French National Research Agency (#ANR-15-CE31-0010) and JHH, AHK, FH,  
582 and RMH thank W.M. Keck Foundation for financial supports.

583

584 **Author contributions** JHH and AHK conceived of the project. JHH compiled and FH  
585 analyzed the paleosol data. JHH and FH performed the simulations; JHH and AHK analyzed  
586 the results. All authors discussed the results and wrote the manuscript.

587

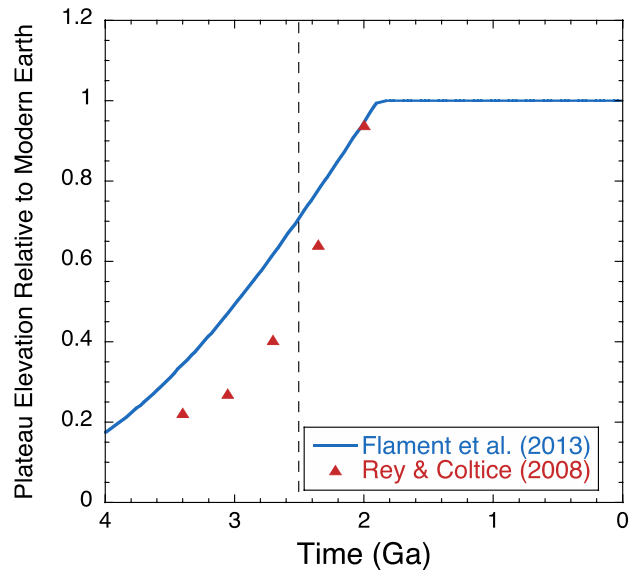
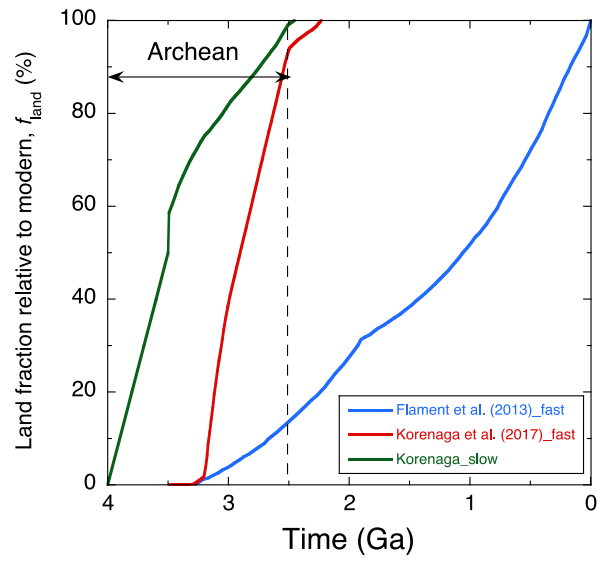
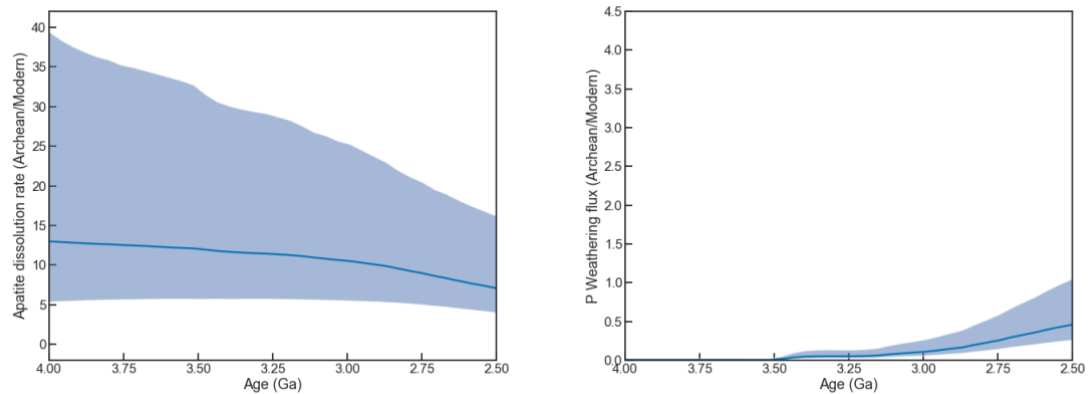


Figure 1. The timing of continental emergence: (a) emergence of continental land above sea level according to Flament et al. (2013) and Korenaga et al. (2017) and (b) ratio of maximum plateau elevation on the Archean Earth relative to today (5520 m).

594



595

596 Figure 2. Continental weathering of phosphorus in the case of slow continental emergence in  
597 the late Archean Eon (Flament et al., 2013, in Figure 1): (a) ratio of acidic dissolution rates of  
598 apatite (rate per unit area) in the Archean relative to today; (b) ratio of weathering flux of  
599 phosphorus in the Archean relative to today. Solid lines show median outputs, and shaded  
600 regions show 95% confidence intervals.

601

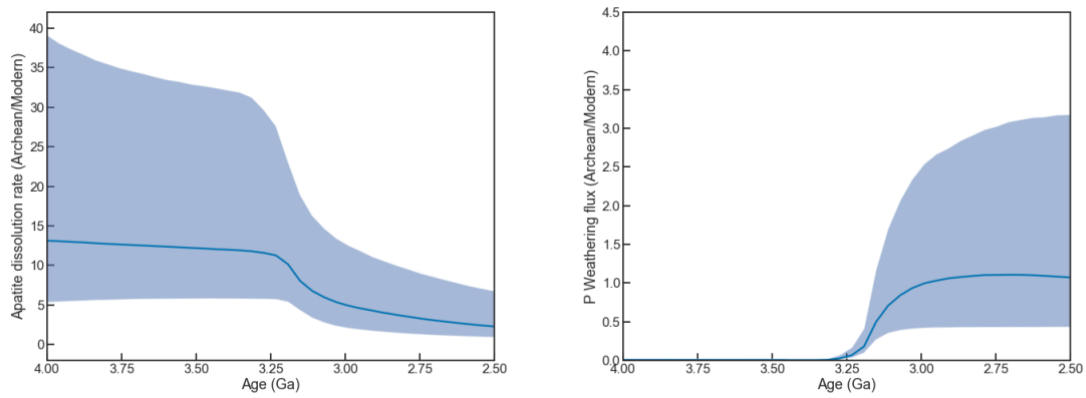
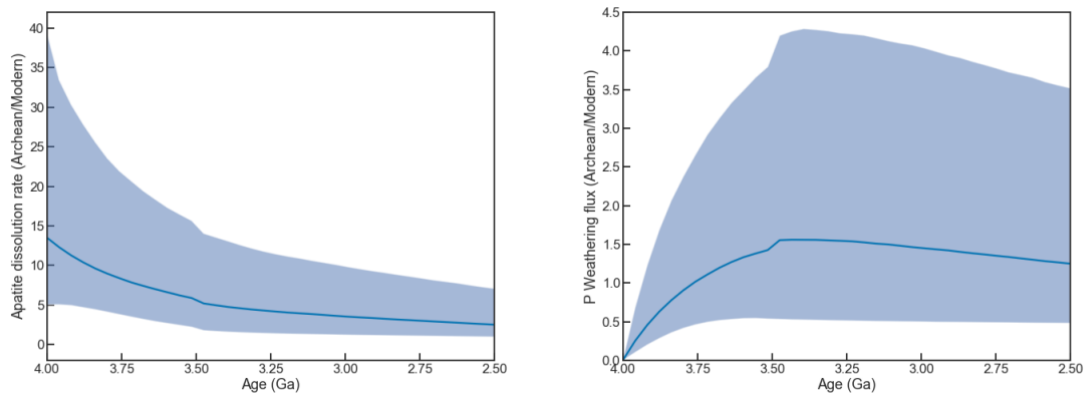


Figure 3. Continental weathering of phosphorus in the case of rapid continental emergence in the late Archean (Korenaga et al., fast in Figure 1): (a) acidic dissolution rates of apatite relative to today;(b) weathering flux of phosphorus relative to today. Solid lines show median outputs, and shaded regions show 95% confidence intervals.



608

609 Figure 4. Continental weathering of phosphorus in the case of rapid continental emergence of  
 610 in the early Archean Eon (Korenaga\_slow in Figure 1): (a) acidic dissolution rates of apatite;  
 611 (b) weathering flux of phosphorus. Solid lines show median outputs, and shaded regions show  
 612 95% confidence intervals.

613

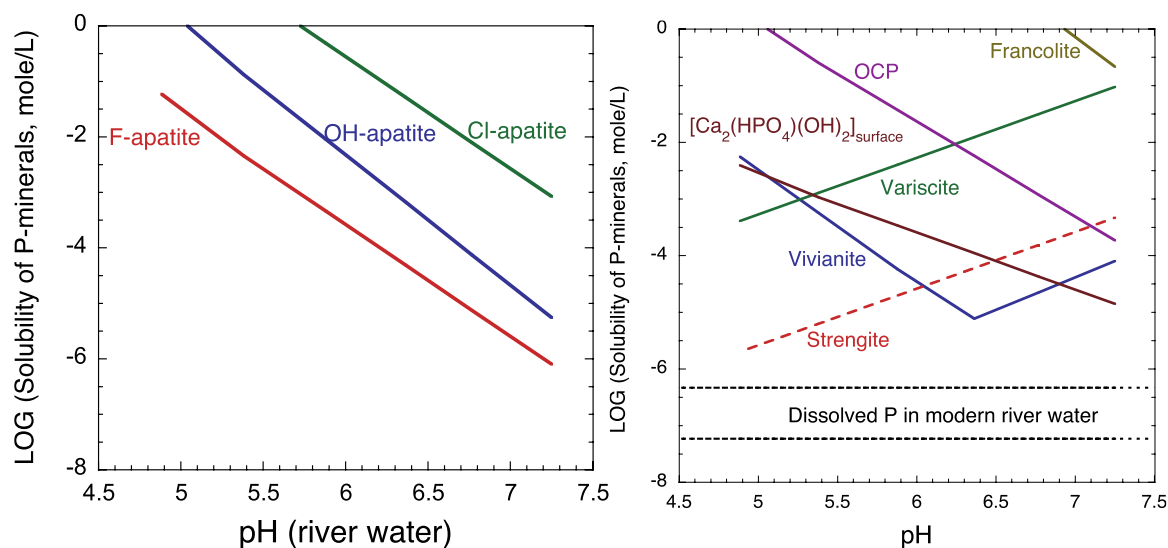
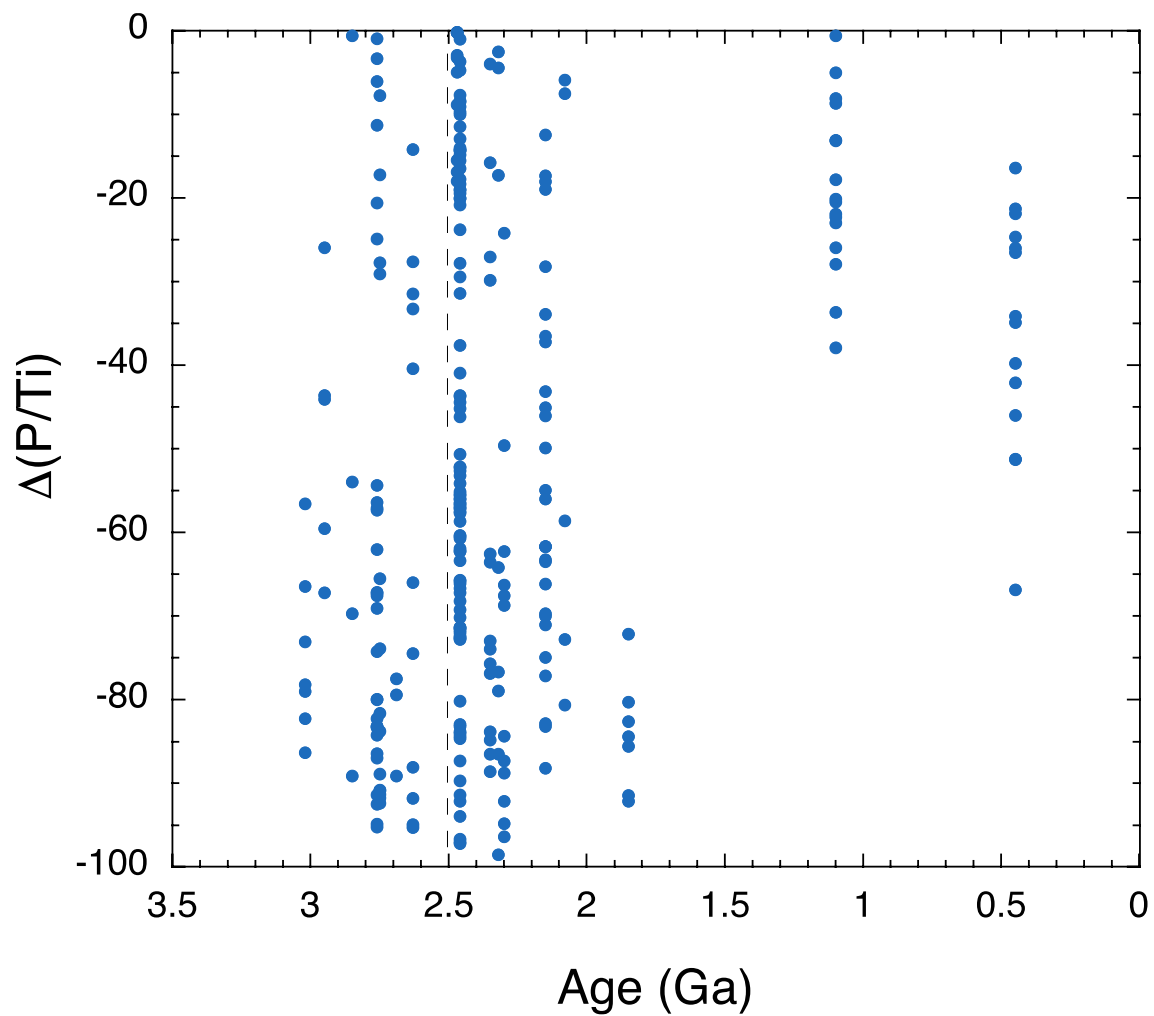


Figure 5. Leaching weathering of phosphorus on the Archean continents. (a) Solubility limits of apatite in the Archean rainwater as a function of pH. (b) Solubility limits of various secondary P-bearing minerals in Archean river water as a function of pH. See **Methods & Materials** and **Table S1** for assumptions on the concentrations of other ions and **Table 1** for thermodynamic data.



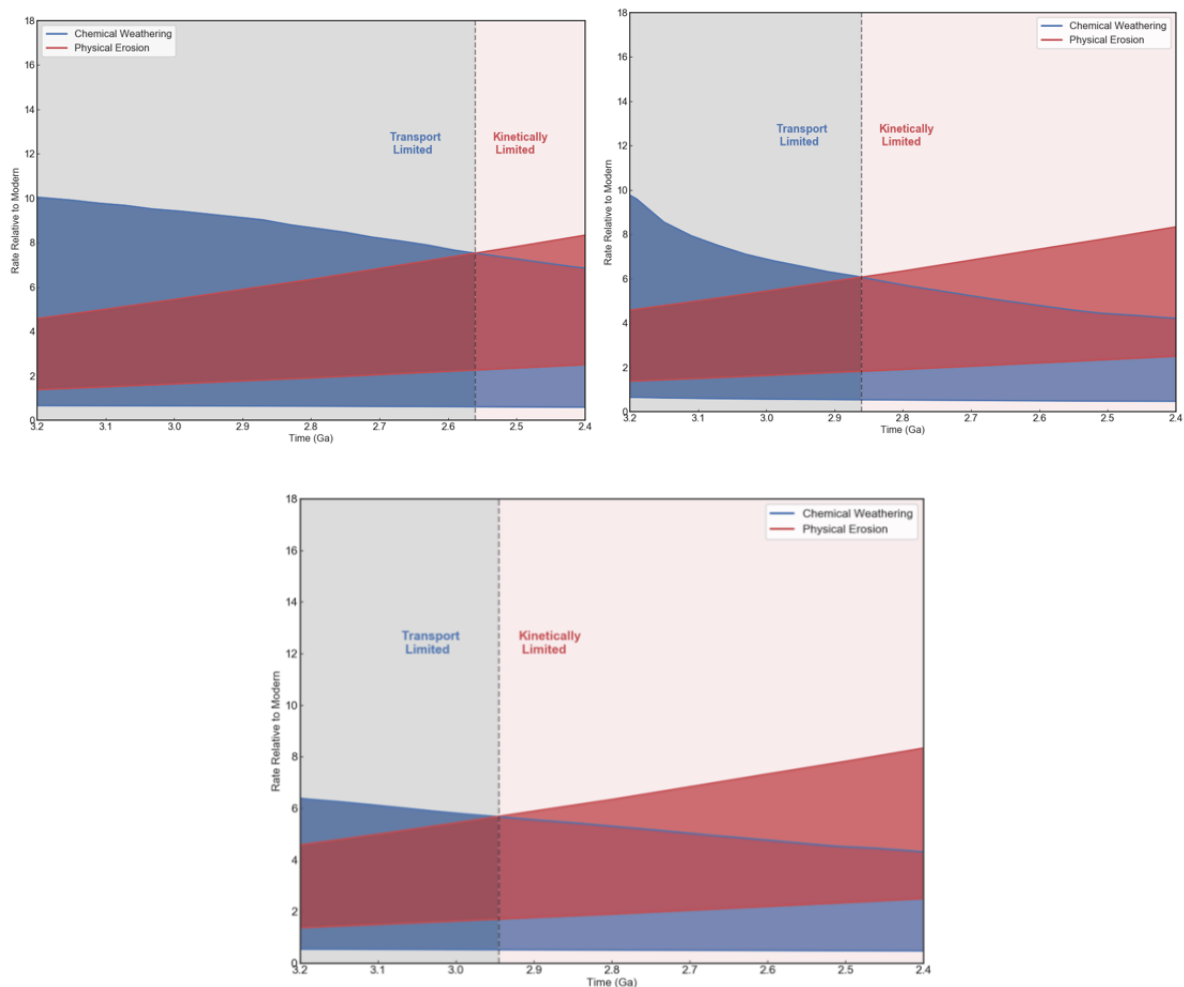
Group 1: (P/Ti)\_Archean  
Group 2: (P/Ti)\_post-Archean

|           | Group 1  | Group 2  |
|-----------|----------|----------|
| Count     | 75       | 212      |
| Mean      | -63.9824 | -48.2789 |
| Variance  | 779.282  | 822.446  |
| Std. Dev. | 27.9156  | 28.6783  |
| Std. Err  | 3.22342  | 1.96963  |

|                    |          |
|--------------------|----------|
| Mean Difference    | -15.7035 |
| Degrees of Freedom | 133      |
| t Value            | -4.1571  |
| t Probability      | < .0001  |

Figure 6. Leaching weathering of P recorded in paleosols. (a) P depletion ( $\Delta P/Ti < 0$ ) relative to bedrock in paleosols; (b) Student's t-test results of Archean and post-Archean paleosols'  $\Delta P/Ti$ .

627



629

630 Figure 7. Relative intensity of chemical and physical weathering on the Archean Earth  
 631 compared with today in the three cases of continental emergence: (a) slow emergence in the  
 632 late Archean; (b) rapid emergence in the late Archean; (c) rapid emergence in the early Archean.  
 633 Blue shaded regions display 95% confidence intervals of the Archean silicate weathering rate  
 634 relative to today.

635



636 Table 1. Solubility reactions of primary and secondary P-bearing minerals in Archean river water.

| Solubility in river water                                   | Combined reaction <sup>a</sup>  | Log K              |
|---|---|--------------------|
| OH-apatite  | $\text{Ca}_5(\text{PO}_4)_3(\text{OH}) + 7\text{H}^+ \rightarrow 5\text{Ca}^{2+} + 3\text{H}_2\text{PO}_4^- + \text{H}_2\text{O}$   | 16.5 <sup>a</sup>  |
| Cl-apatite  | $\text{Ca}_5(\text{PO}_4)_3\text{Cl} + 6\text{H}^+ \rightarrow 5\text{Ca}^{2+} + 3\text{H}_2\text{PO}_4^- + \text{Cl}^-$  | 12.0 <sup>a</sup>  |
| F-apatite   | $\text{Ca}_5(\text{PO}_4)_3\text{F} + 6\text{H}^+ \rightarrow 5\text{Ca}^{2+} + 3\text{H}_2\text{PO}_4^- + \text{F}^-$  | -1.15 <sup>a</sup> |
| Vivianite   | $\text{Fe}_3(\text{PO}_4)_2 \cdot 8\text{H}_2\text{O} + 4\text{H}^+ \rightarrow 3\text{Fe}^{2+} + 2\text{H}_2\text{PO}_4^- + 8\text{H}_2\text{O}$   | 3.31 <sup>b</sup>  |
| Variscite   | $\text{AlPO}_4 \cdot 2\text{H}_2\text{O}_{\text{s}} + \text{H}_2\text{O} \rightarrow \text{Al}(\text{OH})_{3,\text{am}} + \text{H}_2\text{PO}_4^- + \text{H}^+$   | -8.27 <sup>c</sup> |
| Strengite   | $\text{FePO}_4 \cdot 2\text{H}_2\text{O}_{\text{s}} + \text{H}_2\text{O} \rightarrow \text{Fe}(\text{OH})_{3,\text{am}} + \text{H}_2\text{PO}_4^- + \text{H}^+$   | -10.6 <sup>d</sup> |
| $[\text{Ca}_2(\text{HPO}_4)(\text{OH})_2]_{\text{surface}}$ | $\text{Ca}_5(\text{PO}_4)_3(\text{OH}) + 3\text{H}_2\text{O} + \text{H}^+ \rightarrow 2\text{Ca}_2(\text{HPO}_4)(\text{OH})_2 + \text{Ca}^{2+} + \text{H}_2\text{PO}_4^-$   | -2.59 <sup>e</sup> |
| Octacalcium phosphate (OCP)                                 | $\text{Ca}_4\text{H}(\text{PO}_4)_3 \cdot 2.5\text{H}_2\text{O} + 5\text{H}^+ \rightarrow 4\text{Ca}^{2+} + 3\text{H}_2\text{PO}_4^- + 2.5\text{H}_2\text{O}$   | 10.3 <sup>f</sup>  |
| Francolite  | $\text{Ca}_{10}(\text{PO}_4)_{5.5}(\text{CO}_3)_{0.5}\text{F}_{2.5} + 12\text{H}^+ \rightarrow 10\text{Ca}^{2+} + 5.5\text{H}_2\text{PO}_4^- + 0.5\text{CO}_{2,\text{g}} + 2.5\text{F}^- + 0.5\text{H}_2\text{O}$ | 38.0 <sup>g</sup>  |

637 <sup>a</sup>Calculated with SUPCRT92b (Johnson et al., 1992); <sup>b</sup>Calculated with SUPCRT92 and the reported log  $K_{\text{sp,Vivianite}}$  (Al-Borno and Tomson, 1994);  
638 <sup>c</sup>Calculated with SUPCRT92b and the reported log  $K_{\text{sp,Variscite}}$  (Stumm and Morgan, 1996); <sup>d</sup>Calculated with SUPCRT92b, log  $K_{\text{s,Fe}(\text{OH})_3}$  (Liu and  
639 Millero, 1999), and the reported log  $K_{\text{sp,Strengite}}$  (Stumm and Morgan, 1996); <sup>e</sup>Calculated with SUPCRT92b and data from (Fox et al., 1985);  
640 <sup>f</sup>Calculated with SUPCRT92b and data from log  $K_{\text{sp,OCP}}$  (Tung et al., 1988); <sup>g</sup>Calculated with SUPCRT92b and data from log  $K_{\text{sp,Francolite}}$  (Vieillard,  
641 1978).

Table 2. The continental flux of biologically available P (= DIP + DOP + POP + PIP Fe-bound + 20% Aeolian) (Compton et al., 2000) in the late Archean compared with preindustrial time (in 10<sup>10</sup> moles P/yr).

| <b>Riverine Phosphorus</b>                         | <b>Preindustrial</b> | <b>Late Archean</b>   | <b>Bioavailability</b> |
|--|----------------------|-----------------------|------------------------|
| <b>DIP (dissolved inorganic P)</b>                 | 0.97-1.6             | 1.5-30 <sup>a</sup>   | Y                      |
| <b>DOP (dissolved organic P)</b>                   | 0.65                 | 0.1-0.65 <sup>b</sup> | Y                      |
| <b>POP (particulate organic P)</b>                 | 2.9                  | 0.3-2.9 <sup>c</sup>  | Y                      |
| <b>PIP (particulate inorganic P),<br/>Fe-bound</b> | 4.8-9.7              | 0                     | Y                      |
| <b>PIP, detrital</b>                               | 22-39                | 2.2-39 <sup>d</sup>   | N                      |
| <b>Aeolian phosphorus</b>                          | 3.2                  | 0.3-3.2 <sup>e</sup>  | 20% <sup>f</sup>       |
| <b>Total (bioavailable P)</b>                      | 10-15.5              | 4-34                  |                        |

<sup>a</sup>(DIP(modern) + PIP,Fe-bound (modern)) \* p(Archean)/p(Modern); <sup>b</sup>DOP(modern) \* SA(Archean)/SA(Modern); <sup>c</sup>POP(modern) \* SA(Archean)/SA(Modern); <sup>d</sup>PIP,detrital(Modern) \* SA(Archean)/SA(Modern); <sup>e</sup>Aeolian(modern) \* SA(Archean)/SA(Modern); <sup>f</sup>Assume same percentage on the Archean Earth.

## References:

- Al-Borno, A., Tomson, M.B., 1994. The temperature dependence of the solubility product constant of vivianite. *Geochim. Cosmochim. Acta.* **58(24)**, 5373-5378.  
doi:10.1016/0016-7037(94)90236-4
- Arndt, N., 1999. Why was flood volcanism on submerged continental platforms so common in the Precambrian? *Precambrian Res.* **97(3-4)**, 155-164. doi:10.1016/S0301-9268(99)00030-3
- Bataille C. P., Willis A., Yang X. and Liu X. M. (2017) Continental igneous rock composition: A major control of past global chemical weathering. *Sci. Adv.* **3**. Available at: <https://advances.sciencemag.org/content/3/3/e1602183>.
- Berner, R.A., 2004. *The Phanerozoic Carbon Cycle: CO<sub>2</sub> and O<sub>2</sub>*. Oxford University Press Oxford.
- Berner E. K., Berner R. A. and Moulton K. L. (2003) Plants and Mineral Weathering: Present and Past. In *Treatise on Geochemistry* pp. 169–188.
- Bindeman, I.N., Zakharov, D.O., Palandri, J., Greber, N.D., Dauphas, N., Retallack, G.J., Hofmann, A., Lackey, J.S., Bekker, A., 2018. Rapid emergence of subaerial landmasses and onset of a modern hydrologic cycle 2.5 billion years ago. *Nature* **557**, 545–548.  
doi:10.1038/s41586-018-0131-1
- Bjerrum, C.J., Canfield, D.E., 2002. Ocean productivity before about 1.9 Gyr ago limited by phosphorus adsorption onto iron oxides. *Nature* **417**, 159–162. doi:10.1038/417159a
- Blank, C.E., Sanchez-Baracaldo, P., 2010. Timing of morphological and ecological innovations in the cyanobacteria - A key to understanding the rise in atmospheric oxygen. *Geobiology* **8**, 1–23. doi:10.1111/j.1472-4669.2009.00220.x
- Bluth G. J. S. and Kump L. R. (1991) Phanerozoic paleogeology. *Am. J. Sci.* **291**, 284–308.
- Byerly, B.L., Lowe, D.L., Drabon, N., Coble, M.A., Burns, D.H., and Byerly, G.R., 2018.

675 Hadean zircon from a 3.3 Ga sandstone, Barberton greenstone belt, South Africa.  
676 *Geology* **46**, 967-970. doi.org /10.1130 /G45276 .1

677 Campbell, I.H., Davies, D.R., 2017. Raising the continental crust. *Earth Planet. Sci. Lett.* **460**,  
678 112-122. doi:10.1016/j.epsl.2016.12.011

679 Compton, J., Mallinson, D., Glenn, C.R., Filippelli, G., Föllmi, K., Shields, G., Zanin, Y.,  
680 2000. Variations in the Global Phosphorus Cycle. *Mar. Authigenes. From Glob. to*  
681 *Microb.* 21–33. doi:10.2110/pec.00.66.0021

682 Cox, G.M., Lyons, T.W., Mitchell, R.N., Hasterok, D., Gard, M., 2018. Linking the rise of  
683 atmospheric oxygen to growth in the continental phosphorus inventory. *Earth Planet.*  
684 *Sci. Lett.* **489**, 28–36. doi:https: 10.1016/j.epsl.2018.02.016

685 Culling W. E. H. (1960) Analytical Theory of Erosion. *J. Geol.* **68**, 336–344.

686 Culling W. E. H. (1963) Soil Creep and the Development of Hillside Slopes. *J. Geol.* **71**,  
687 127–161.

688 Derry, L.A., 2015. Causes and consequences of mid-Proterozoic anoxia. *Geophys. Res. Lett.*  
689 **42(20)**, 8538-8546 doi:10.1002/2015GL065333

690 Deshmukh, A.N., Wadaskar, P.M., Malpe, D.B., 1995. Fluorine in environment: A review.  
691 *Gondwana Geol. Mag* **9**, 1–20.

692 Drabon N., Lowe D. R., Byerly G. R. and Harrington J. A. (2017) Detrital zircon  
693 geochronology of sandstones of the 3.6-3.2 Ga Barberton greenstone belt: No evidence  
694 for older continental crust. *Geology* **45**, 803–806.

695 Drever, J.I., 1994. The effect of land plants on weathering rates of silicate minerals.  
696 *Geochim. Cosmochim. Acta.* **58(10)**, 2325-2332. doi:10.1016/0016-7037(94)90013-2

697 Edmond, J.M., Palmer, M.R., Measures, C.I., Grant, B., Stallard, R.F., 1995. The fluvial  
698 geochemistry and denudation rate of the Guayana Shield in Venezuela, Colombia, and  
699 Brazil. *Geochim. Cosmochim. Acta* **59**, 3301–3325. doi:10.1016/0016-7037(95)00128-

700 M

701 Ernst, W.G., Sleep, N.H., Tsujimori, T., 2016. Plate-tectonic evolution of the Earth: bottom-  
702 up and top-down mantle circulation. *Can. J. Earth Sci.* **53(11)**, 1103-1120.

703 doi:10.1139/cjes-2015-0126

704 Flament, N., Coltice, N., Rey, P.F., 2013. The evolution of the  $^{87}\text{Sr}/^{86}\text{Sr}$  of marine  
705 carbonates does not constrain continental growth. *Precambrian Res.* **229**, 177–188.

706 doi:10.1016/j.precamres.2011.10.009

707 Flament, N., Coltice, N., Rey, P.F., 2008. A case for late-Archaean continental emergence  
708 from thermal evolution models and hypsometry. *Earth Planet. Sci. Lett.* **275(3-4)**, 326-

709 336. doi:10.1016/j.epsl.2008.08.029

710 Fox, L.E., Sager, S.L., Wofsy, S.C., 1985. Factors controlling the concentrations of soluble  
711 phosphorus in the Mississippi estuary. *Limnol. Oceanogr.* **30(4)**, 826-832.

712 doi:10.4319/lo.1985.30.4.0826

713 Gaillardet, J., Viers, J., Dupré, B., 2014. 7.7 - Trace Elements in River Waters A2 - Turekian,

714 Heinrich D. Holland Karl K, in: *Treatise on Geochemistry (Second Edition)*. Elsevier,

715 Oxford, pp. 195–235. doi:http://dx.doi.org/10.1016/B978-0-08-095975-7.00507-6

716 Gough, D.O., 1981. Solar interior structure and luminosity variations. *Sol. Phys.* **74**, 21–34.

717 doi:10.1007/BF00151270

718 Guidry, M.W., Mackenzie, F.T., 2003. Experimental study of igneous and sedimentary

719 apatite dissolution: Control of pH, distance from equilibrium, and temperature on

720 dissolution rates. *Geochim. Cosmochim. Acta.* **67(16)**, 2949-2963. doi:10.1016/S0016-

721 7037(03)00265-5

722 Guidry, M.W., Mackenzie, F.T., 2000. Apatite weathering and the Phanerozoic phosphorus

723 cycle. *Geology* **28**, 631–634. doi: 10.1130/0091-

724 7613(2000)028<0631:Awatpp>2.3.Co;2

725 Gyssels, G., Poesen, J., Bochet, E., Li, Y., 2005. Impact of plant roots on the resistance of  
 726 soils to erosion by water: A review. *Prog. Phys. Geogr.* **29**(2), 189-217.  
 727 doi:10.1191/0309133305pp443ra

728 Hao, J., Sverjensky, D.A., Hazen, R.M., 2019. Redox states of Archean surficial  
 729 environments: The importance of H<sub>2,g</sub> instead of O<sub>2,g</sub> for weathering reactions. *Chem.*  
 730 *Geol.* **521**, 49-58. doi:10.1016/j.chemgeo.2019.05.022

731 Hao, J., Sverjensky, D.A., Hazen, R.M., 2017a. Mobility of nutrients and trace metals during  
 732 weathering in the late Archean. *Earth Planet. Sci. Lett.* **471**, 148–159.  
 733 doi:10.1016/j.epsl.2017.05.003

734 Hao, J., Sverjensky, D.A., Hazen, R.M., 2017b. A model for late Archean chemical  
 735 weathering and world average river water. *Earth Planet. Sci. Lett.* **457**, 191–203.  
 736 doi:10.1016/j.epsl.2016.10.021

737 Hart M. H. (1978) The evolution of the atmosphere of the earth. *Icarus* **33**, 23–39.

738 Hartmann J., Moosdorf N., Lauerwald R., Hinderer M. and West A. J. (2014) Global  
 739 chemical weathering and associated p-release - the role of lithology, temperature and  
 740 soil properties. *Chem. Geol.* **363**, 145–163.

741 Hawkesworth, C.J., Kemp, A.I.S., 2006. Evolution of the continental crust. *Nature.*  
 742 **443**(7113), 811. doi:10.1038/nature05191

743 House, W.A., 2003. Geochemical cycling of phosphorus in rivers. *Appl. Geochemistry* **18**,  
 744 739–748. doi:10.1016/S0883-2927(02)00158-0

745 Jadamec M. A., Turcotte D. L. and Howell P. (2007) Analytic models for orogenic collapse.  
 746 *Tectonophysics* **435**, 1–12.

747 Johnson, J.W., Oelkers, E.H., Helgeson, H.C., 1992. SUPCRT92: A software package for  
 748 calculating the standard molal thermodynamic properties of minerals, gases, aqueous  
 749 species, and reactions from 1 to 5000 bar and 0 to 1000 °C. *Comput. Geosci.* **18**, 899–

750 947. doi:10.1016/0098-3004(92)90029-Q  
 751 Jones, C., Nomosatryo, S., Crowe, S.A., Bjerrum, C.J., Canfield, D.E., 2015. Iron oxides,  
 752 divalent cations, silica, and the early earth phosphorus crisis. *Geology* **43**, 135–138.  
 753 doi:10.1130/G36044.1  
 754 Kasting J. F., Zahnle K. J., Pinto J. P. and Young A. T. (1989) Sulfur, ultraviolet radiation,  
 755 and the early evolution of life. *Orig. Life Evol. Biosph.* **19**, 95–108.  
 756 Kipp, M.A., Stüeken, E.E., 2017. Biomass recycling and Earth’s early phosphorus cycle. *Sci.*  
 757 *Adv.* 3. doi:10.1126/sciadv.aao4795  
 758 Knoll A. H. and Beukes N. J. (2009) Introduction: Initial investigations of a Neoarchean shelf  
 759 margin-basin transition (Transvaal Supergroup, South Africa). *Precambrian Res.* **169**,  
 760 1–14.  
 761 Korenaga, J., Planavsky, N.J., Evans, D.A.D., 2017. Global water cycle and the coevolution  
 762 of the Earth’s interior and surface environment. *Philos. Trans. R. Soc. A Math. Phys.*  
 763 *Eng. Sci.* **375(2094)**:20150393.. doi:10.1098/rsta.2015.0393  
 764 Krissansen-Totton, J., Arney, G.N., Catling, D.C., 2018. Constraining the climate and ocean  
 765 pH of the early Earth with a geological carbon cycle model. *Proc. Natl. Acad. Sci.*  
 766 201721296. doi:10.1073/pnas.1721296115  
 767 Krissansen-Totton, J., Buick, R., Catling, D.C., 2015. A statistical analysis of the carbon  
 768 isotope record from the Archean to phanerozoic and implications for the rise of oxygen.  
 769 *Am. J. Sci.* **315(4)**, 275-316. doi:10.2475/04.2015.01  
 770 Kump, L.R., Barley, M.E., 2007. Increased subaerial volcanism and the rise of atmospheric  
 771 oxygen 2.5 billion years ago. *Nature.* **448(7157)**, 1033. doi:10.1038/nature06058  
 772 Laakso, T.A., Schrag, D.P., 2018. Limitations on Limitation. *Global Biogeochem. Cycles* **32**,  
 773 486–496. doi:10.1002/2017GB005832  
 774 Lee, C.-T.A., Thurner, S., Paterson, S., Cao, W., 2015. The rise and fall of continental arcs:

775 Interplays between magmatism, uplift, weathering, and climate. *Earth Planet. Sci. Lett.*  
 776 **425**, 105–119. doi:10.1016/j.epsl.2015.05.045  
 777 Lee, C.T.A., Caves, J., Jiang, H., Cao, W., Lenardic, A., McKenzie, N.R., Shorttle, O., Yin,  
 778 Q. zhu, Dyer, B., 2018. Deep mantle roots and continental emergence: implications for  
 779 whole-Earth elemental cycling, long-term climate, and the Cambrian explosion. *Int.*  
 780 *Geol. Rev.* **60(4)**, 431–448. doi:10.1080/00206814.2017.1340853  
 781 Lenton T. M., Daines S. J. and Mills B. J. W. (2018) COPSE reloaded: An improved model  
 782 of biogeochemical cycling over Phanerozoic time. *Earth-Science Rev.* **178**, 1–28.  
 783 Liu, X., Millero, F.J., 1999. The solubility of iron hydroxide in sodium chloride solutions.  
 784 *Geochim. Cosmochim. Acta.* **63(19-20)**, 3487–3497. doi:10.1016/S0016-  
 785 7037(99)00270-7  
 786 Lowe D. R. and Byerly G. R. (1999) *Geologic evolution of the Barberton greenstone belt,*  
 787 *South Africa.*, Geological Society of America.  
 788 Marks, M.A.W., Markl, G., 2017. A global review on agpaitic rocks. *Earth-Science Rev.* **173**,  
 789 229–258. doi:10.1016/j.earscirev.2017.06.002  
 790 Molnar, P., 2018. Gravitational Potential Energy per Unit Area as a Constraint on Archean  
 791 Sea Level. *Geochemistry, Geophys. Geosystems.* **19(10)**, 4063–4095.  
 792 doi:10.1029/2018GC007766  
 793 Neaman, A., Chorover, J., Brantley, S.L., 2005. Element mobility patterns record organic  
 794 ligands in soils on early Earth. *Geology* **33**, 117–120. doi:10.1130/G20687.1  
 795 Nocita B. W. (1989) Sandstone petrology of the Archean Fig Tree Group, Barberton  
 796 greenstone belt, South Africa: tectonic implications. *Geology* **17**, 953–956.  
 797 Owen T., Cess R. D. and Ramanathan V. (1979) Enhanced CO<sub>2</sub> greenhouse to compensate  
 798 for reduced solar luminosity on early Earth [5]. *Nature* **277**, 640–642.  
 799 Pasek, M., Lauretta, D., 2008. Extraterrestrial flux of potentially prebiotic C, N, and P to the



800 early earth. *Orig. Life Evol. Biosph.* **38**(1), 5-21. doi:10.1007/s11084-007-9110-5

801 Planavsky, N.J., Rouxel, O.J., Bekker, A., Lalonde, S. V, Konhauser, K.O., Reinhard, C.T.,  
802 Lyons, T.W., 2010. The evolution of the marine phosphate reservoir. *Nature* **467**, 1088–  
803 1090. doi:10.1038/nature09485

804 Pons, M.L., Fujii, T., Rosing, M., Quitté, G., Télouk, P., Albarède, F., 2013. A Zn isotope  
805 perspective on the rise of continents. *Geobiology*. **11**(3), 201-214.  
806 doi:10.1111/gbi.12030

807 Porder, S., Ramachandran, S., 2013. The phosphorus concentration of common rocks-a  
808 potential driver of ecosystem P status. *Plant Soil*. **367**(1-2), 41-55. doi:10.1007/s11104-  
809 012-1490-2

810 Reinhard, C.T., Planavsky, N.J., Gill, B.C., Ozaki, K., Robbins, L.J., Lyons, T.W., Fischer,  
811 W.W., Wang, C., Cole, D.B., Konhauser, K.O., 2017. Evolution of the global  
812 phosphorus cycle. *Nature* **541**, 386–389. doi:10.1038/nature20772

813 Rey, P.F., Coltice, N., 2008. Neoproterozoic lithospheric strengthening and the coupling of  
814 Earth's geochemical reservoirs. *Geology* **36**, 635–638. doi:10.1130/G25031A.1;

815 Roberts, N.M.W., Spencer, C.J., 2015. The zircon archive of continent formation through  
816 time. *Geol. Soc. London, Spec. Publ.* **389**(1), 197-225. doi:10.1144/SP389.14

817 Ronov A. B. (1982) The Earth's Sedimentary Shell (Quantitative Patterns of its Structure,  
818 Compositions, and Evolution): The 20th V.I. Vernadskiy Lecture, March 12,1978. *Int.*  
819 *Geol. Rev.* **24**, 1313–1363.

820 Ruttenberg, K.C., 2013. The Global Phosphorus Cycle, in: *Treatise on Geochemistry: Second*  
821 *Edition*. doi:10.1016/B978-0-08-095975-7.00813-5

822 Rye, R., Holland, H.D., 1998. Paleosols and the evolution of atmospheric oxygen: A critical  
823 review. *Am. J. Sci.* **298**, 621–672. doi:10.2475/ajs.298.8.621

824 Satkoski, A.M., Lowe, D.R., Beard, B.L., Coleman, M.L., Johnson, C.M., 2016. A high

continental weathering flux into Paleoarchean seawater revealed by strontium isotope  
analysis of 3.26 Ga barite. *Earth Planet. Sci. Lett.* **454**, 28-35.  
doi:10.1016/j.epsl.2016.08.032

Schlesinger, W.H., Bernhardt, E.S., 2013. *Biogeochemistry: an analysis of global change*.  
Academic press.

Spencer, C.J., Partin, C.A., Kirkland, C.L., Raub, T.D., Liebmann, J., Stern, R.A., 2019.  
Paleoproterozoic increase in zircon  $\delta_{18}\text{O}$  driven by rapid emergence of continental crust.  
*Geochim. Cosmochim. Acta.* **257**, 16-25. doi:10.1016/j.gca.2019.04.016

Stüeken, E.E., Catling, D.C., Buick, R., 2012. Contributions to late Archaean sulphur cycling  
by life on land. *Nat. Geosci.* **5**, 722–725. doi:10.1038/ngeo1585

Stumm, W., Morgan, J.J., 1996. *Aquatic Chemistry: Chemical Equilibria and Rates in  
Natural Waters*, 3<sup>rd</sup> edition. Wiley.

Taylor S. R. and McLennan S. M. (1985) *The continental crust: Its composition and  
evolution.*, Blackwell Scientific Pub., Palo Alto, CA, United States.

Trower, E.J., Lowe, D.R., 2016. Sedimentology of the ~3.3 Ga upper Mendon Formation,  
Barberton Greenstone Belt, South Africa. *Precambrian Res.* **281**, 473-494.  
doi:10.1016/j.precamres.2016.06.003

Tsukamoto, Y., Kakegawa, T., Graham, U., Liu, Z.-K., Ito, A., Ohmoto, H., 2018. Discovery  
of Ni-Fe Phosphides in the 3.46 Ga-Old Apex Basalt: Implications on the Phosphate  
Budget of the Archean Oceans. *Goldschmidt Abstr.* 2577.

Tung, M.S., Eidelman, N., Sieck, B., Brown, W.E., 1988. Octacalcium Phosphate Solubility  
Product from 4 to 37 °C. *J. Res. Natl. Bur. Stand.* **93**, 613-624. doi:10.6028/jres.093.153

Tyrrell T. (1999) The relative influences of nitrogen and phosphorus on oceanic primary  
production. *Nature* **400**, 525–531.

Van Kranendonk, M., 2006. Volcanic degassing, hydrothermal circulation and the flourishing

850 of early life on Earth: A review of the evidence from c. 3490-3240 Ma rocks of the  
 851 Pilbara Supergroup, Pilbara Craton, Western Australia. *Earth-Sci. Rev.* **74**, 197– 240.  
 852 doi:10.1016/j.earscirev.2005.09.005  
 853 Viehmann, S., Bau, M., Hoffmann, J.E., Münker, C., 2018. Decoupled Hf and Nd isotopes in  
 854 suspended particles and in the dissolved load of Late Archean seawater. *Chem. Geol.*  
 855 **483**, 111-118. doi:10.1016/j.chemgeo.2018.01.017  
 856 Vieillard, P., 1978. Géochimie des phosphates. Étude thermodynamique. Application à la  
 857 genèse et à l'altération des apatites. Persée-Portail des revues scientifiques en SHS.  
 858 West, J., Galy, A., Bickle, M., 2005. Tectonic and climatic controls on silicate weathering.  
 859 *Earth Planet. Sci. Lett.* **235**, 211–228. doi:10.1016/j.epsl.2005.03.020  
 860 Withers, P.J.A., Jarvie, H.P., 2008. Delivery and cycling of phosphorus in rivers: A review.  
 861 *Sci. Total Environ.* **400(1-3)**, 379-395. doi:10.1016/j.scitotenv.2008.08.002  
 862 Zhou, P., Luukkanen, O., Tokola, T., Nieminen, J., 2008. Effect of vegetation cover on soil  
 863 erosion in a mountainous watershed. *Catena* **75**, 319–325.  
 864 doi:10.1016/j.catena.2008.07.010  
 865